WELDING RESEARCH

SUPPLEMENT TO THE WELDING JOURNAL, MARCH 1975

Sponsored by the American Welding Society and the Welding Research Council

Welding of an Advanced High Strength Titanium Alloy

Metallurgical investigation points the way to solution of high strength titanium welding problems

BY M. A. GREENFIELD AND D. S. DUVALL

ABSTRACT. Many recently developed high strength titanium alloys do not possess the inherent good weldability of previous alloys in this material system. Difficulties have been encountered in achieving satisfactory weldment mechanical properties in several of these alloys. The present investigation was conducted to study the metallurgical response of one of these materials, Ti-6246, to arc welding. The goal was to identify the causes for inferior properties in advanced titanium alloy weldments and to provide guidelines for improved processing procedures to correct welding difficulties.

Gas tungsten-arc welds made on 0.125 in. thick sheet were evaluated metallographically and with hardness, bend, and tensile tests to characterize their properties in the as-welded condition and after various postweld heat treatments. Gleeble synthetic heat-affected zone specimens were utilized to more fully study this weldment region. These tests revealed that the weld and near heat-affected zone regions were extremely hard and brittle as welded and after a normal postweld stress relief. Studies showed that this was caused by rapid auto-aging of an orthorhombic martensite phase formed during the weld thermal cycle. Solution heat treating after welding removed the orthorhombic martensite but failed to substantially improve weld ductility. Films of alpha phase precipitated at prior beta grain boundaries during the solution heat treatment were responsible for the low weld ductility in this condition. Based upon these results, a new postweld heat treatment was established which successfuly increased weld ductility by favorably altering the weld and heat-affected zone alpha precipitation. This approach and others suggested by this investigation appear to be promising methods for improving the weldability of advanced titanium alloys.

M. A. GREENFIELD is Technical Manager for Joining, Air Force Materials Laboratory, Metals and Ceramics Division, Wright-Patterson AFB, Ohio 45433. D. S. DUVALL is Research Metallurgist, Advanced Materials R&D Laboratory, Pratt & Whitney Aircraft, Middletown, Conn. 06458.

Paper was presented at the 55th AWS Annual Meeting held at Houston, Texas, during May 6-10, 1974.

Introduction

Structural components of titanium and titanium alloys are widely utilized in both airframe and gas turbine engine construction because of their high strength-to-density ratios. Welding is often employed on these airframe and engine components in order to reduce costs, simplify construction, or achieve superior performance. It is well known that porosity, contamination, and embrittlement problems can be encountered when welding these chemically active alloys. However, these difficulties can be prevented by proper preweld cleaning methods and adequate protection of the material during welding. Furthermore, because of the inherent good weldability of many of today's titanium alloys, weldment cracking is usually not a problem during fabrication and near base metal mechanical properties can be achieved without the need for unique filler metal compositions, weld energy input controls and postweld heat treatment cycles.

The ever increasing performance demand of advanced aircraft and engine systems has led to the need for titanium alloys with greater strength and more heat resistance, and several new alloys have been developed. Many applications require that they be employed in welded construction. Unfortunately, initial investigations suggest that some of these alloys do not have the easy weldability inherent in previous alloys.

The increased amounts of beta stabilizing elements (e.g., molybdenum, iron, vanadium, and others) in advanced titanium alloys has tended to reduce weldability. The

"alpha-lean beta" Ti-6Al-2Sn-4Zr-2Mo* alloy exhibits inconsistent arc welded mechanical properties due to sensitivity to small variations in weld cooling rates (Ref. 1). The alpha+beta Ti-6Al-6V-2Sn alloy has poor ductility (Refs. 2, 3) and toughness (Ref. 4) when conventionally fusion welded and heat treated. Likewise, unsatisfactory ductility has been encountered in fusion weldments in the metastable beta Ti-8Mo-8V-2Fe-3Al alloy (Ref. 5).

These studies have shown that it can be difficult to achieve satisfactory properties when welding these high strength titanium alloys. It has become necessary to develop unique weld and heat treat procedures to control the alpha-beta phase transformations and precipitation reactions responsible for the deleterious weld properties in these materials. For instance, it has been shown that control of weld heating and cooling rates by preheating could improve the toughness of Ti-6Al-6V-2Sn welds (Ref. 4). Experiments have also been conducted to match fusion zone properties to those of the base metal by weld chemistry control with dissimilar filler metals (Ref. 6). However, this approach cannot solve attendant heat-affected zone difficulties.

A thorough understanding of the metallurgical response to welding of these advanced titanium alloys is required if the causes of inferior heat-affected zone and weld metal properties are to be identified and corrected. Some recent studies have successfully used this approach. Gas tungsten-arc weldment ductilities in the Ti-6Al-6V-2Sn and Ti-8Mo-8V-2Fe-3Al alloys were significantly improved by unique postweld heat treatments (Refs. 3, 7). These heat treatments produced heat-affected zone alpha phase morphologies which are considerably more fracture resistant than the microstructures obtained in the as-welded or conventionally postweld heat treated conditions. A similar approach was used to increase poor heat-affected zone impact strengths in 60 mm thick electroslag welds of an experimental Ti-Al-V-Mo-Cr-Fe-Zr alloy (Ref. 8). In addition, thermomechanical processing involving postweld rolling has been employed to favorably alter intragranular alpha precipitation in Ti-8Mo-8V-2Fe-3Al weld metal (Ref. 9).

The present investigation was conducted to gain a better understanding of the welding behavior of advanced titanium alloys by studying the welding metallurgy of the alpha-beta Ti-6Al-2Sn-4Zr-6Mo (Ti-6246) alloy. This high strength material is considerably stronger at elevated temperatures than contemporary alpha-beta titanium alloys. At the time this study was initiated, little experience existed on joining the Ti-6246 alloy. However, because of its high hardener content and quantity of beta stabilizing elements, it was felt that the Ti-6246 alloy would present more of an arc welding problem than other advanced titanium materials including the Ti-6Al-6V-2Sn alloy previously discussed.

Studies on wrought Ti-6246 have shown that the parent alloy can exhibit wide ranging strengths, ductilities, and fracture toughness depending upon heat treatment (Ref. 10). Cooling rates from high solution heat treatment temperatures appear to be especially critical in relation to plane strain fracture toughness and tensile properties. This behavior suggested that the Ti-6246 alloy would be very sensitive to weld thermal cycles.

In the initial phase of this work, the microstructural and mechanical property characteristics of Ti-6246 gas tungsten-arc welds were examined in the as-welded condition and after conventional heat treatments. These results identified deficiencies in heat-affected zone and weld metal properties. A more detailed study was then undertaken, including use of Gleeble synthetic specimen techniques, to determine microstructure/property relationships which were responsible for the weldment properties. Based on these results, various solutions were evaluated for improving the weldability of this advanced titanium alloy.

Material and Procedures

The chemical analysis of the heat of Ti-6246 alloy employed in this investigation is listed in Table 1. All material was taken from 36 in. wide by 0.125 in. thick sheet supplied in an annealed condition (1600 F/15 min/air cool). Prior to welding or other processing, all specimens were solution heat treated at 1700 F (25 F below the beta transus for this particular heat) for 1 hour in argon followed by an air cool. Welded samples were evaluated in the as-welded condition and after various postweld heat treatments. Welds given a direct age/stress relief were heat treated in argon at 1100 F/8 h followed by an air cool. Other welded samples were given a full heat treatment by solutioning at 1700 F/1 h/air cool and aging at 1100 F/8 h/air cool. The microstructure of the base metal given the full heat treatment (solution plus age) is shown in Fig. 1.

To prepare for welding, the heat treated specimens were pickled in a HNO_3-HF acid solution to remove any surface contamination. Gas tungsten-arc welding was conducted in an evacuable controlled atmosphere chamber with argon as the shielding gas. Full penetration bead-on-plate autogeneous welds were made using 10 V dcsp, 150 A, and 5.5 ipm travel speed (16.4 kJ/in. energy input). Current and travel speed parameters were altered on a few welds to vary energy input over a range of 10-20 kJ/in.

In order to study the response of the alloy to welding in more detail, a series of synthetic heat-affected zones were created using a Gleeble. Sheet specimens 3 in. long × 0.5 in. wide × 0.125 in. thick were heated to various peak temperatures along weld thermal cycles. The synthetically created heat-affected zone regions in the center portions of the samples were subsequently examined metallographically or tested mechanically.

Bend tests, hardness measurements and tensile tests were used to characterize the mechanical behavior of the welded sheet specimens and Gleeble samples. Bend tests were performed at room temperature using a 3-point guided bend fixture with a 0.25 in. (2T) radius plunger. The bend specimens were approximately 2 in. long, 0.5 in. wide and 0.125 in. thick. Welded specimens were bent with the welds in the longitudinal direction (perpendicular to the bend axis) and the face (top surface) of the weld in tension. Prior to bending, the specimens were mechanically ground and polished to remove the weld bead reinforcement and then pickled to eliminate any surface contamination. Bend tests were terminated at the onset of cracking, when possible, to allow identification of crack initiation sites. Hardness measurements were made on metallographic specimens using a Vickers hardness tester with a 5 kg load. Room temperature tensile tests were conducted with the test specimen geometries illustrated in Fig. 2. In the welded specimens, the longitudinal test direction was parallel to the weld axis. The miniature specimen design (Fig. 2b) was employed for testing fusion zone material and synthetic heat-affected zones.

Specimens for light metallography were prepared by polishing through 600A paper followed by fine polishing with alumina slurries. The samples were then swab etched in a 50 part lactic acid, 30 part HNO_3, 2 part HF solution. Thin foils for transmission electron microscopy were prepared by the Air Force Materials Laboratory and at Polytechnic Institute of New York (PINY) by Dr. Ernest Levine using standard solutions (Ref. 11) but with a potentiostatic power source. An x-ray diffractometer with pulse height analyzer was used to measure the degree of phase orthorhombicity of

This nomenclature indicates nominal compositions in weight percent.

each zone of the weldment at PINY. Scanning electron microscopy was employed for fractographic analyses of broken bend and tensile specimens.

Results

Metallographic examination of as-welded Ti-6246 bead-on-plate welds showed that a wide range of microstructures existed across the weld zone, Fig. 3. These heat-affected and fusion zone microstructures reflected the effects of rapid heating and cooling weld thermal cycles on an allotropic material. In heat-affected zone regions farthest from the fusion zone, the equiaxed primary alpha particles (white etching phase in Fig. 3) had been partially dissolved by exposure to temperatures slightly below the beta transus*. These partially solutioned alpha particles were surrounded by a matrix of fine transformed beta phase. The higher peak temperatures reached in the middle heat-affected zone produced increased dissolution of the base metal microstructure. In these regions, the structure was characterized by ghost islands of affected alpha particles in a transformed beta matrix.

All remnants of the prior equiaxed alpha phase were erased in the high temperature heat-affected zone locations nearest to the fusion zone. These regions exhibited a fine transformed beta structure in large prior beta grains. The fusion zone contained a similar structure, although the transformed beta morphology was more heterogeneous as a result of solute segregation during solidification. The grain size of the prior beta grains in the heat-affected zone increased in the classical fashion as the fusion zone was approached. Likewise, the fusion zone contained large columnar prior beta grains typical of a solidification structure.

Welded specimens given a direct age/stress relief of 1100 F/8 h after welding exhibited the microstructures shown in Fig. 4. It was apparent that some additional metallurgical changes had taken place in the heat-affected zones during this heat treatment. However, it was difficult to ascertain the exact nature of these changes with the light microscope.

A more dramatic effect (Fig. 5) was produced by fully heat treating the welded specimens at 1700 F/1 h (solution) plus 1100 F/8 h (age). Coarse alpha platelets were formed throughout the prior beta grains in the higher temperature near-heat-affected zone and fusion zone regions during the postweld solution part of the treatment (Figs. 5a, 5b). In addition, large amounts of alpha phase precipitated along the prior beta grain boundaries.

The middle and lower temperature far-heat-affected zone regions, Figs. 5c, 5d, contained a heterogeneous distribution of coarse alpha platelets in a fine structured matrix. In the middle heat-affected zone, alpha platelets in the Widmanstätten relationship also formed at the sites of former equiaxed alpha particles which were dissolved during welding. This was also evident in the lower temperature

The beta transus for this heat of material was experimentally determined to be 1725± 5 F.

Table 1 — Chemical Analysis of Ti-6246 Sheet Used in This Study, wt. %

Titanium	Bal.
Aluminum	5.9
Tin	2.0
Zirconium	4.1
Molybdenum	5.8
Iron	0.11
Carbon	0.026
Nitrogen	0.009
Hydrogen	0.004
Oxygen	0.11

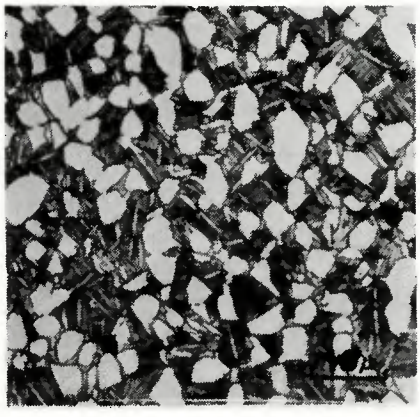

Fig. 1 — Microstructure of fully heat treated Ti-6246 sheet employed in this program. X1000, not reduced

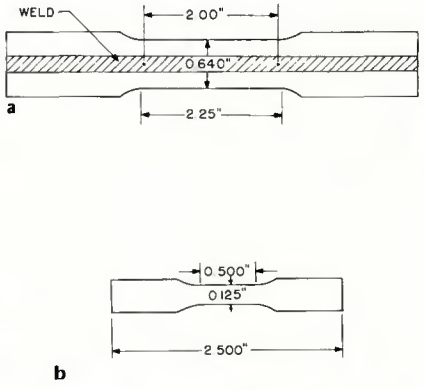

Fig. 2 — Specimens used for tensile testing. (a) Full-size specimen for welded samples. (b) Miniature specimen for fusion-zone and synthetic heat-affected zone tests

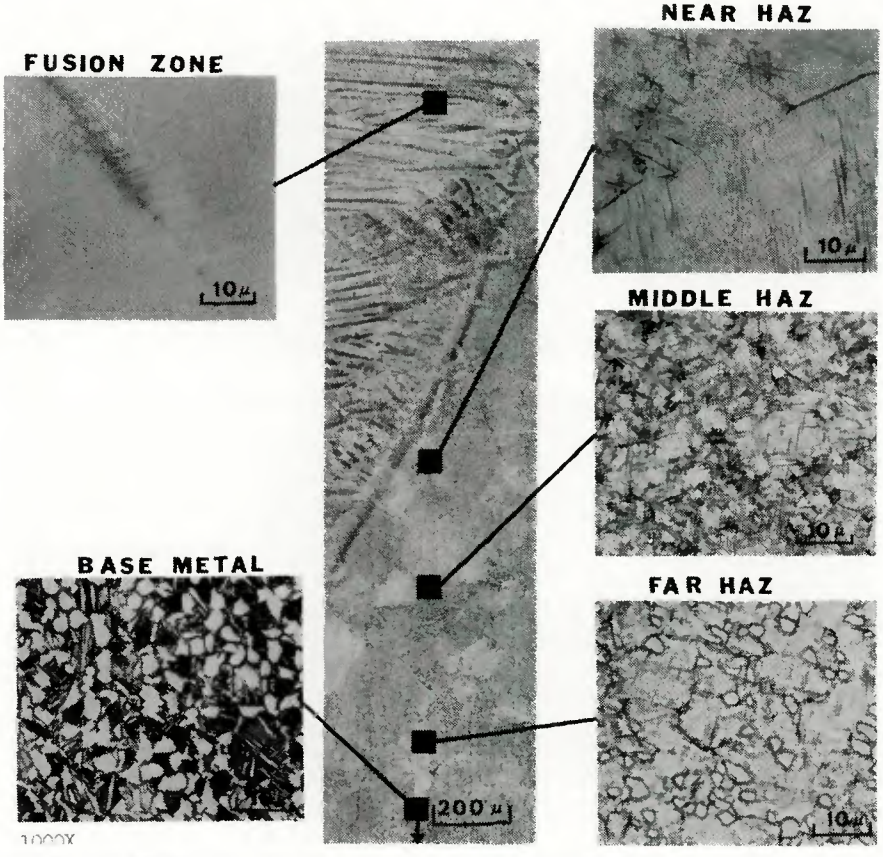

Fig. 3 — As-welded microstructure of gas-tungsten arc weld in Ti-6246 alloy, reduced 29%

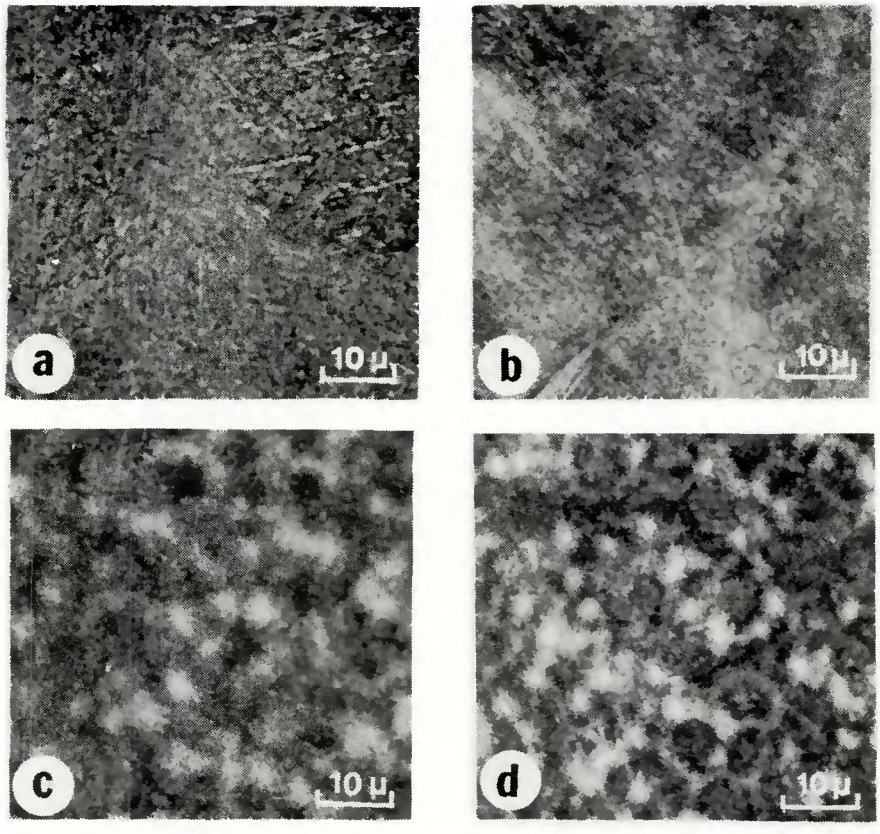

Fig. 4 — Microstructure of Ti-6246 weldment given a direct age/stress relief at 1100 F/8 h AC. (a) Fusion zone, (b) Near heat-affected zone, (c) Middle heat-affected zone, (d) Far heat affected zone. X1000, not reduced

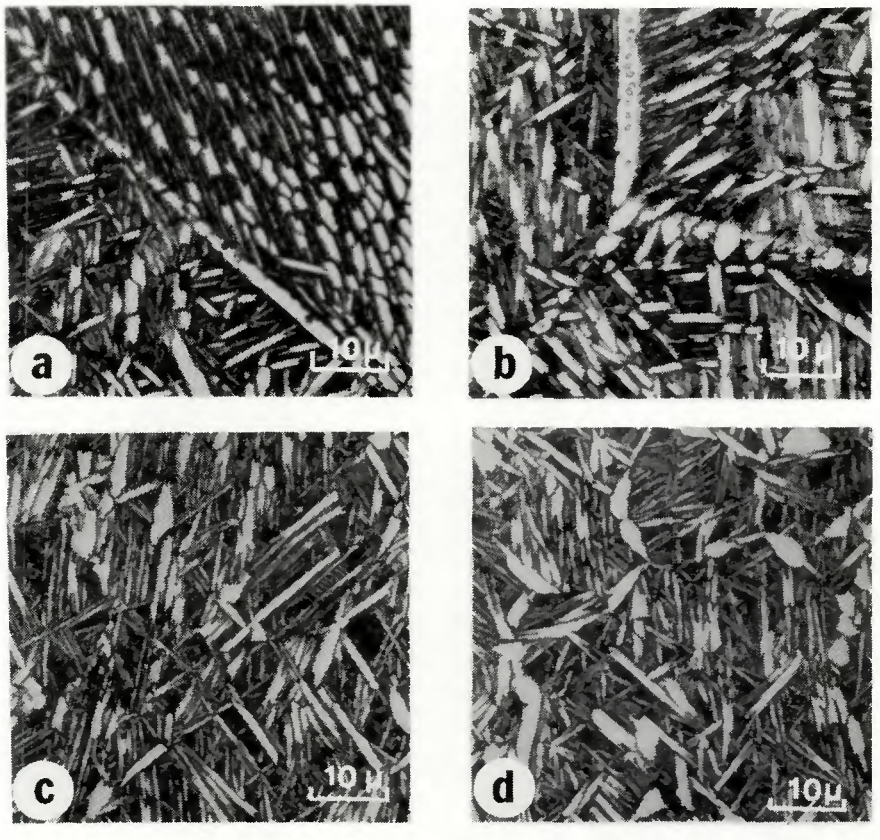

Fig. 5 — Microstructure of Ti-6246 weldment given a full heat treatment of 1700 F/1 h/AC + 1100 F/8 h/AC. (a) Fusion zone, (b) Near heat-affected zone, (c) Middle heat-affected zone, (d) Far heat-affected zone. X1000, not reduced

Table 2 — Ti-6246 Fusion Zone Properties

Postweld condition	Room-temperature tensile tests Y.S., ksi	T.S., ksi	El., %
As welded	—	187	0.4
Direct age/ Stress Relief 1100 F/8 h/AC	—	184	0.3
Full H.T. 1700 F/1 h/AC+ 1100 F/8 h/AC	159	165	2.4

heat-affected zone, where the alpha platelets nucleated and grew from former equlaxed alpha particles which were only partially dissolved during the weld thermal cycle.

It was anticipated that the variety of microstructural changes induced by welding and postweld heat treatment would strongly affect mechanical behavior in this alloy. A series of microhardness traverses were taken across Ti-6246 weldments which were in the above conditions. The results were quite different from what is generally experienced in arc welded alpha-beta titanium alloys such as Ti-6Al-4V (Ref. 12) and Ti-6Al-6V-2Sn (Ref. 3). As shown in Fig. 6, the weld zone and near-heat-affected zone in the as-welded condition were extremely hard when compared to the base metal (460 VHN vs 360 VHN). Moreover, the direct age/stress relief not only failed to lower these hardnesses but extended this region farther into the heat-affected zone. Only after a full solution and age heat treatment did the hardness values level out across the weld.

Longitudinal bend tests conducted on welded specimens in these three conditions also demonstrated that mechanical properties were strongly altered. As-welded specimens cracked with essentially no macroscopic deformation at a bend angle of 0 deg. Specimens given the direct age also failed in a brittle manner at an average bend angle of about 10 deg. The fully heat treated weld specimens exhibited an average bend angle of about 20 deg although each showed intergranular fracture across most of the weld affected region. Fully heat treated base metal bend specimens (with the same sheet orientation) failed at angles of about 30 deg in similar bend tests. Examination of the fractured bend specimens indicated that cracking initiated in the fusion zone or high temperature portion of the heat-affected zone in all welded samples tested.

In order to ascertain the meaning of these hardness and bend data and to quantitatively determine the actual properties of each weldment zone, a series of subsize fusion zone and Gleeble simulated heat-affected zone

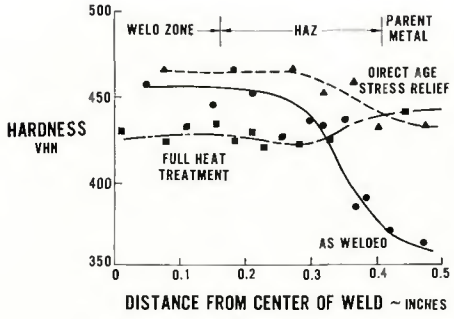

Fig. 6 — Microhardness traverses across Ti-6246 welds

specimens was prepared and tensile tested at room temperature. The tensile results of the fusion zone specimens are shown in Table 2. It can be seen that in both the as-welded and direct aged/stress relieved condition the tensile strength was extremely high with unacceptably low ductility. In the fully heat treated condition, the fusion zone had base metal strength but also possessed low ductility.

Examination of the fracture surfaces of these specimens with a scanning electron microsope revealed that the low ductility fractures could be attributed to the failure mode. In the as-welded and direct aged/stress relieved conditions, the fracture surfaces showed a transgranular cleavage type and a brittle precipitate failure respectively, Fig. 7. In contrast, fully heat treated fusion zone specimens exhibited an intergranular failure with ductile dimpling at the grain boundary surfaces, Fig. 8. Subsequent metallography demonstrated that the change in fracture mode and the low tensile elongation in the fusion zone were related to microstructural phase distributions. This will be discussed later in detail.

Figure 9 shows the difference in microstructures which was found in synthetically created heat-affected zones as a result of different peak temperatures. These Gleeble structures closely resembled the actual heat-affected zone of the as-welded sheet. Peak temperatures below 1725 F were characterized by partially dissolved primary alpha particles surrounded by transformed beta, Fig. 9a. In cases where the beta transus was exceeded, such as in Fig. 9b, a structure of transformed beta phase resulted. Consistent with previous investigations (Ref. 13), x-ray diffraction analysis showed no retained beta phase.

The results of tensile tests on various Gleeble specimens are plotted in Fig. 10. It was observed that the higher the peak temperature of the heat-affected zone, the higher the strength level and the lower the ductility. In particular, these specimens

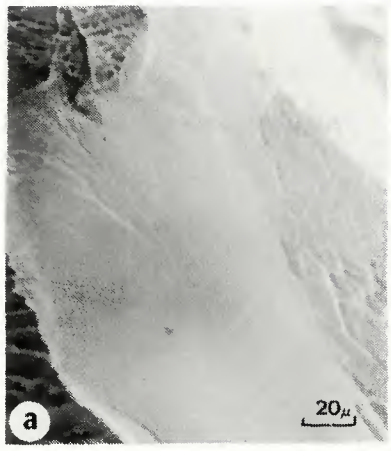

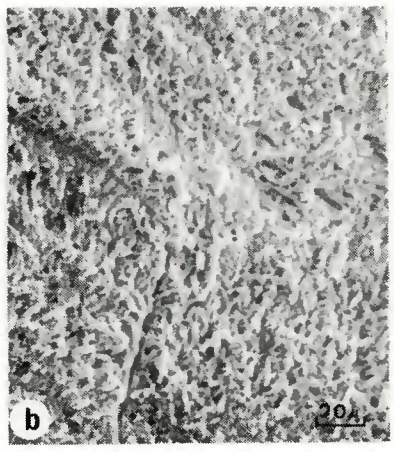

Fig. 7 — Ti-6246 fusion zone fracture surfaces showing brittle transgranular failure mode. (a) As welded, (b) Direct age/stress relief at 1100 F/8 h/AC. X500, reduced 33%

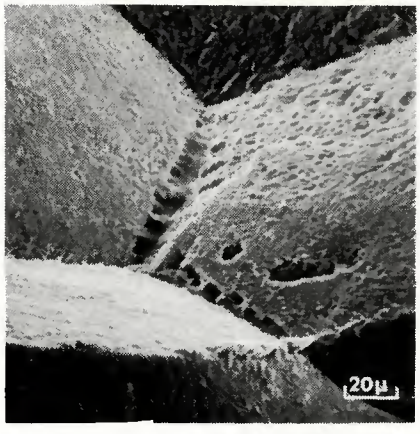

Fig. 8 — Ti-6246 fusion zone fracture in solution heat treated and aged specimen showing intergranular failure with ductile dimpling at grain boundaries. X500, reduced 35%

heated above the beta transus were characterized by extremely high strength and low ductility. This correlated with the trends apparent in the microhardness traverses and the observation that the higher temperature heat-affected zone was a location for crack initiation in bend tests.

Discussion

Individual testing of the fusion zones and simulated heat-affected zones showed that the high hardness profile in Fig. 6 is related to the peak temperature attained in a given area during welding. Areas which were heated above the beta transus during welding exhibited abnormally high strength levels.

In order to determine the cause of these high strength levels, fusion zone and near-heat-affected zone samples were studied by electron microscopy and x-ray diffraction. Examination revealed that an orthorhombic martensite phase (α'') was formed as the beta transformation product upon cooling following welding. The dark

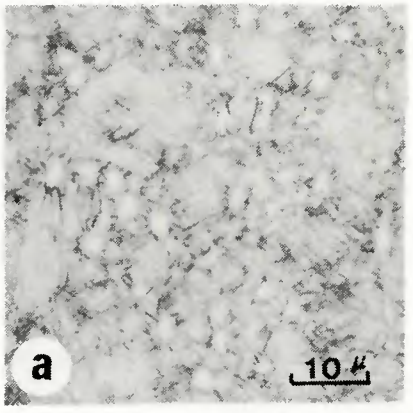

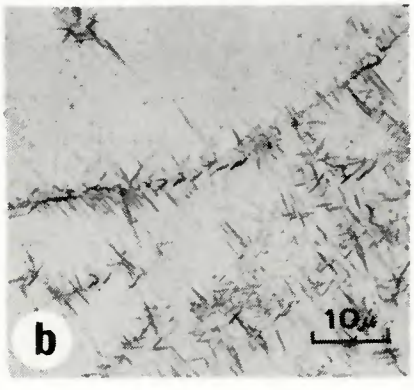

Fig. 9 — Ti-6246 synthetic heat affected zone specimens. (a) Cycled to 1700 F indicated peak temperature, (b) Cycled to 2000 F indicated peak temperature. X1000, not reduced

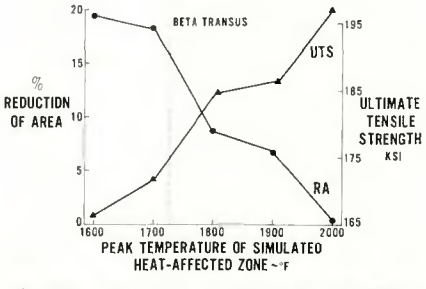

Fig. 10 — Room temperature tensile properties of Ti-6246 synthetic heat affected zone specimens

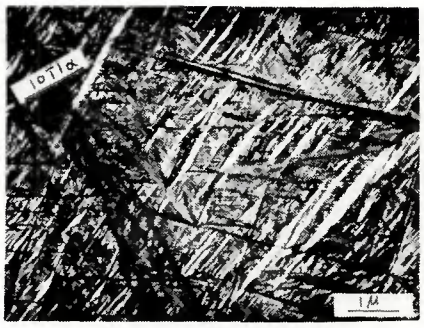

Fig. 11 — Electron micrograph of Ti-6246 synthetic heat-affected zone. Dark field on 1011 α rellection showing twinned orthorhombic martensite. X18,000, reduced 62%

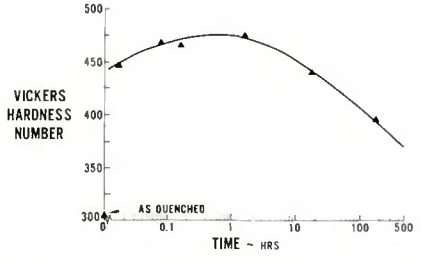

Fig. 12 — 1100 F isothermal aging curve for beta quenched Ti-6246 material (From Ref. 13)

field electron micrograph in Fig. 11 illustrates internally twinned orthorhombic martensite platelets observed in a Gleeble heat-affected zone specimen. This martensite phase occurs in the Ti-6246 and is unlike the normal hexagonal martensite found in other titanium systems (Ref. 14). The α'' martensite is soft in the unaged condition as are all titanium martensites. However, what makes this martensite unique in the case of welding is its ability to rapidly age to extremely high strength levels. Aging occurs by the precipitation of beta phase in the highly twinned martensite, thereby effectively locking slip and inhibiting deformation (Refs. 13, 15). This results in the material with very high yield strength. Figure 12 (reproduced from Ref. 13) demonstrates that aging at 1100 F for as little as 10 seconds increases the beta quenched alloy's hardness from 310 VHN to 450 VHN. It is therefore not unreasonable to expect that a similar effect would be encountered due to auto aging on cooling after welding.

In order to determine if this indeed was the case, Gleeble specimens were heated to 2000 F and 1700 F and cooled at various cooling rates. The data are presented in Table 3. It can be seen that the specimens heated above the beta transus and cooled at 1000 F/s possessed low hardness, 295 VHN, equivalent to the as-quenched hardness in Fig. 12. However, cooling at 60 F/s (more

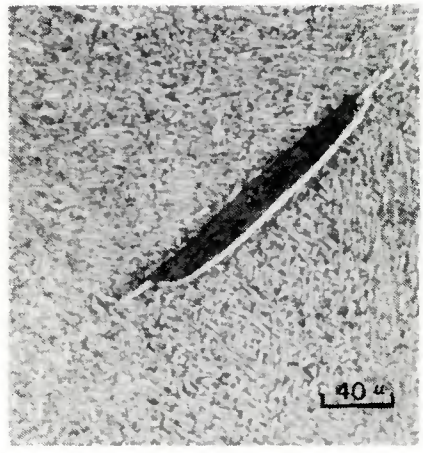

Fig. 13 — Void nucleation and growth at grain boundary alpha in the near heat-affected zone of a Ti-6246 weldment tensile specimen. X250, reduced 21%

characteristic of GTA welding of ⅛ in. plate) resulted in a hardness of 445 VHN. This also is similar to the Fig. 12 curve data at 10 seconds aging. Hence, the high hardness of the as-welded near-heat-affected and fusion zones can be attributed to the formation of orthorhombic martensite and its subsequent aging on cooling.

Gleeble specimens heated to a peak temperature in the alpha-beta phase field, 1700 F, exhibited only moderate hardness in the "as-welded" condition. This structure (Fig. 9) was characterized as a combination of conventionally aged beta phase (strengthening by alpha precipitate through nucleation and growth) and some aged orthorhombic martensite. In fact, the entire hardness curve of Fig. 6 in the heat-affected zone can be related to the amount of aged orthorhombic martensite present. The near-heat-affected zone was heated above the beta transus and consisted of all aged α'' with resultant high hardness. As the peak temperature dropped below the beta transus with increasing distance from the fusion zone, there was a corresponding decrease in the amount of α'' and an increase in aged beta. Since the conventional beta aging reaction is less effective and slower than the aging of the α'', these regions had lower hardness.

Finally, in the unaffected base metal, the hardness and structure were indicative of the preweld alpha plus beta solution treatment and slow-cool consisting of a structure of precipitated alpha in a beta matrix. This was in agreement with Cias (Ref. 16) who showed that cooling rates below approximately 10 F/s in the Ti-6246 alloy avoided the formation of orthorhombic martensite; the beta phase transformed by nucleation and growth of alpha precipitates only.

A standard titanium postweld direct age/stress relief treatment was not suitable for overcoming this deleterious α'' microstructure produced by welding. This is not unexpected from the above discussion and the aging response shown in Fig. 12. The direct age/stress relief heat treatment does nothing more than further the aging reaction of the structure. Figure 12 shows that eight hours is not sufficient time for significant overaging to occur in the α'' rich fusion and near-heat-affected zone. In addition, this treatment resulted in an increase in hardness, Fig. 6, of the far-heat-affected zone and the base material. This is a result of the conventional α precipitation aging of the preweld solution treated material.

Since a range of peak temperatures and cooling rates occurs during the welding process, it appeared that a controllable solution and age cycle after welding would be beneficial. It would not only result in the elimination of orthorhombic martensite and achievement of base metal strengths but also the elimination of strength variation across the weldment. In fact, the microhardness traverse in Fig. 6 for the fully heat treated material showed just that.

However, as with the Table 2 fusion zone results, fully heat treated bead-on-plate weldments possessed low ductility, exhibiting less than 4% elongation and less than 9% RA in a longitudinal tensile specimen. The reason for the low ductility can be attributed to the formation of the grain boundary alpha phase in the near heat-affected zone and fusion zone during the 1700 F solution treatment. At this temperature, only 25 F below the beta transus, the driving force for alpha precipitation was low and hence the beta grain boundaries represented the most favored sites for nucleation.

As has been shown in studies on wrought alpha-beta titanium alloys (Ref. 17), this continuous network of a soft alpha phase, Fig. 5a, 5b, severely degrades the ductility of the material. This is a consequence of the ability of this alpha phase to readily deform by slip due to its Burgers' relationship with the surrounding beta matrix, i.e., $\{110\}_\beta \parallel (0001)_\alpha$, $<111>_\beta \parallel <1120>_\alpha$ and form voids at the alpha/beta interface. These voids can then grow at low stress levels by progressive slip at the void tip until they reach a critical size for fracture.

Figure 13 is a photomicrograph of the heat-affected zone of a weldment unloaded just prior to failure. A large void is clearly seen at the grain boundary alpha phase/beta matrix interface. Rapid void growth early in the straining process promotes intergranular fracture (e.g., Fig. 8) and hence limits the achievable ductility. A

similar phenomenon has been reported in metastable beta titanium alloys (Ref. 7).

Methods for Improving Weldability

This investigation identified the metallurgical causes of the poor weldability of the Ti-6246 alloy. This alloy in the as-welded and direct aged/stress relieved condition is unacceptable due to brittleness from the autotempering of the orthorhombic martensite. A solution and age after welding does eliminate the martensite problem but creates another problem by the formation of a grain boundary alpha network prone to subsequent low ductility intergranular failure.

The high strength level and low ductility of the fusion zone can be altered by choosing a suitable filler metal and therefore is tractable. What must be improved is the ductility of the heat-affected zone. There are two possible approaches: (1) preheat and post heat control to achieve cooling rates which will eliminate the formation of orthorhombic martensite or (2) an improved postweld heat treatment at some intermediate temperature at which grain boundary alpha formation is limited. The second approach is more desirable in that it is not sensitive to part geometry and was therefore examined in this study.

A postweld time-temperature cycle was sought which would effectively eliminate the detrimental α'' without concurrently precipitating the undesirable grain boundary alpha phase. The temperature for such a cycle had to be far enough below the beta transus to insure adequate supersaturation for uniform intragranular alpha precipitation. This would minimize heterogeneous alpha formation at prior beta grain boundaries. However, the heat treatment temperature also had to be high enough to either overage or dissolve the undesirable α'' martensite.

To find the desired postweld heat treatment, welded specimens were heat treated for various times over a range of temperatures from 1300 F to 1600 F, air cooled, and then aged at 1100 F. The most successful postweld heat treatment was at 1400 F/8 h + 1100 F/8 h. This cycle yielded no preferential grain boundary alpha in either the heat-affected zone or fusion zone. The microstructure, shown in Fig. 14, is characterized by Widmanstätten alpha in aged beta. At this temperature, the driving force for precipitation is sufficiently great to cause this type of uniform precipitation instead of the more heterogeneous grain boundary alpha phase. Since there is no continuous path for failure, tensile ductilities approaching base metal levels were achieved in welds given this intermediate postweld heat treatment, Table 4.

These results are encouraging and demonstrate the benefits which can be achieved by manipulation of weldment microstructures. Further work is needed to completely optimize postweld heat treatments for the Ti-6246 alloy and to fully match these cycles to base metal requirements. Likewise, experimentation to explore the effects of weld process variations (e.g., preheat and postheat control) would be useful to determine possible benefits from this approach. Nevertheless, the data from this study suggest that it will be possible to weld many of the advanced, high strength titanium alloys provided weldment microstructure/property relationships are understood and controlled.

Conclusions

1. Gas tungsten-arc welds in the Ti-6246 alloy were extremely hard and brittle in the as-welded condition and following normal direct age/stress relief heat treatments. A full solution + age postweld heat treatment reduced hardness but failed to substantially improve ductility.

2. The cause for the hard, brittle condition of these welds was the formation and rapid auto-aging of orthorhombic martensite in the weld and heat-affected zone on cooling from welding. A normal direct age/stress relief postweld heat treatment only extended this reaction.

3. Solution heat treatments after welding removed the deleterious orthorhombic martensite. However, they caused heterogeneous precipitation of continuous alpha films along prior beta grain boundaries in weld heat-affected regions.

4. An intermediate postweld heat treatment was developed which was successful in improving the weldability of the Ti-6246 alloy. This heat treatment eliminated the orthorhombic martensite while producing uniform alpha precipitation throughout the weld and heat-affected zone.

Acknowledgments

The authors wish to thank Messrs. M. Murphy, C. M. Wickstrand, and A. R. Geary of Pratt & Whitney Aircraft and Mr. N. L. Harruff of the Air Force Materials Laboratory for their assiduous efforts in preparing, testing, and helping to analyze the experimental specimens used in this investigation. In addition, we appreciate those portions of the electron microscopy and x-ray diffraction analyses conducted during this program by Drs. E. Levine and M. Young at the Polytechnic Institute of New York.

References

1. Mitchell, D. R., and Tucker, T. J., "The Properties and Transformation Characteristics in Welds in Ti-6Al-2Sn-4Zr-2Mo Titanium Alloy," *Welding Journal,* 48 (1), Jan. 1969, Res. Suppl., 23-s to 33s.

2. Schwenk, W., Kaehler, W. A., and Kennedy, J. R., "Weldability of Titanium Alloy Sheets 6Al-6V-2Sn and 8Al-1Mo-1V," *Welding Journal,* 46 (2), Feb. 1967, Res. Suppl., 64-s to 73-s.

3. Simpson, R. P., and Wu, K. C., "Microstructure — Property Control With Postweld Heat Treatment in Ti-6Al-6V-2Sn," *Welding Journal,* 53 (1), Jan. 1974, Res. Suppl., 13-s to 18-s.

4. Lewis, R. E., and Wu, K. C., "A Study of Weld Heat-Affected Zones in the Titanium 6Al-6V-2Sn Alloy," *Welding Journal,* 42 (6), June 1963, Res. Suppl., 241-s to 249-s.

5. Hatch, W., "Development of Welding Practices for Titanium Alloy 8Mo-8V-2Fe-3Al," Technical Report to Army Materials and Mechanics Research Agency, Watertown, Ma., AMMRC PTR-73-4, March 1973.

6. Mitchell, D. R., and Fiege, N. G., "Welding of Alpha-Beta Titanium Alloy in One Inch Plate," *Welding Journal,* 46 (5), May 1967, Res. Suppl., 193-s to 202-s.

7. Greenfield, M. A., and Pierce, C. M.,

Table 3 — Effect of Cooling Rate on Heat-Affected-Zone Hardness

Gleeble peak temp., F	Cooling rate F/s	VHN
2000	1000	295
2000	60	445
2000	25	450
—	—	—
1700	60	400

Table 4 — Intermediate Postweld Heat Treatment for Ti-6246 Weldments

	1400 F/8 h + 1100 F/8 h			
	Y.S., ksi	T.S., ksi	El., %	R.A. %
Weld	154	163	7.3	16.5
Base metal	162	172	12.5	18.8

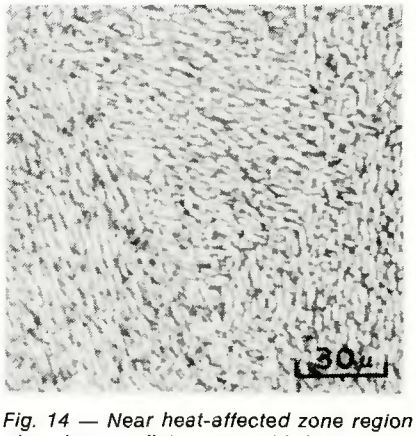

Fig. 14 — Near heat-affected zone region after intermediate postweld heat treatment at 1400 F/8 h/AC + 1100 F/8 h/AC. X400, not reduced

"Postweld Aging of a Metastable Beta Titanium Alloy," *Welding Journal,* 52 (11), Nov. 1973, Res. Suppl., 524-s to 527-s.

8. Grabin, V. R., and Cerkasov, N. I., "Structure and Properties of the Heat Affected Zone in the Electroslag Welding of a High Strength Titanium Alloy," *Avt. Svarka,* No. 9, 20-23, (1973).

9. Greenfield, M. A., and Haggard, D. K., "Thermomechanical Processing of a Welded Metastable Beta Titanium Alloy," *Welding Journal,* 53 (8), Aug. 1974, Res. Suppl., 339-s to 342-s.

10. Hall, J. A., Pierce, C. M., Ruckle, D. L., and Sprague, R. A., "Property-Microstructure Relationship in the Ti-6Al-2Sn-4Zr-6Mo Alloy," *Mat'l Science Eng.* Vol. 9, p 197, (1972).

11. Williams, J. C., and Blackburn, M. J., "The Preparation of Thin Foils of Titanium Alloys," *Trans. AIME,* 239, p 287, 1967.

12. Banas, C. M., "Electron Beam, Laser Beam and Plasma Arc Welding Studies," NASA Report CR-132386, NASA Langley Research Center, March, (1974).

13. Young, M., Levine, E., and Margolin, H., "The Aging Behavior of Orthorhombic Martensite in Ti-6246," *Met. Trans.* Vol. 5, p 1891, (1974).

14. Williams, J. C., and Hickman, B. S., "Tempering Behavior of Orthorhombic Martensite in Titanium Alloys," *Met. Trans.,* Vol. 1, p 2648, (1970).

15. Young, M., Levine, E., and Margolin, H., "Deformation Behavior of Alpha, Beta and Martensite in Ti-6246 Alloy," presented at ASM/TMS-AIME "Material Science Symposium," Detroit, Oct. 21, 1974.

16. Cias, W. W., "Phase Transformational Kinetics, Microstructures and Hardenability of the Ti-6246 Alloy," Climax Molybdenum Report RP-27-71-02, March 6, 1972.

17. Greenfield, M. A., and Margolin, H., "The Mechanism of Void Formation, Void Growth and Tensile Fracture in an Alloy Consisting of Two Ductile Phases," *Met. Trans.,* Vol. 3, p 2649, (1972).

WRC Bulletin No. 198
SEPT. 1974

"Secondary Stress Indices for Integral Structural Attachments to Straight Pipe"

by W. G. Dodge

"Stress Indices at Lug Supports on Piping Systems"

by E. C. Rodabaugh, W. D. Dodge and S. E. Moore

This report presents a simplified method for calculating the stresses induced in straight pipe by thrust and moment loadings applied to lugs and other integral attachments. Following the philosophy of the nuclear power piping portion of Section III of the ASME Boiler and Pressure Vessel Code, appropriate secondary stress indices are defined. A simple and conservative formula for computing the stress indices is developed using analytical results as a guide. A comparison is made between experimental stress indices and those obtained using the simplified analysis procedure developed here as well as the more complex analysis procedures of *Welding Research Council Bulletin 107* (WRC-107 method). The method is extended to attachments having a variety of cross sections.

Stress indices and the appropriate simplified design formulas are developed for analyzing integral lug attachments on straight pipe according to the philosophy of Section III of the ASME Boiler and Pressure Vessel Code for Class I Piping Systems. Indices are developed for the evaluation of primary stresses, primary-plus-secondary stresses, and peak stresses due to internal pressure in the pipe for radial thrust and transverse shear forces and torsional and bending moment loads acting on the lug; and for a thermal gradient between the pipe and the lug. The indices for thrust and bending moment loads are based on an extensive parameter study and are represented by simple formulas that may be used directly by designers and/or incorporated into codes and standards. From comparisons with other methods of analysis these formulas are considered to be more accurate and easier to use. Indices for the other loadings are based in part on strength-of-materials theory and information in the literature. Specific recommendations are made for incorporating the stress indices and design formulas into the ASME Code. As an example, a simple pipe support design is analyzed using the recommended formulas.

Publication of these papers was sponsored by the Pressure Vessel Research Committee of the Welding Research Council. The price of WRC Bulletin 198 is $6.00. Orders should be sent to the Welding Research Council, 345 East 47th Street, New York, N.Y. 10017.